

C

[Crown Copyright Reserved] R 55236

AIR MINISTRY.

FOR OFFICIAL USE.

T. 2680.

AERONAUTICAL RESEARCH COMMITTEE.

REPORTS AND MEMORANDA No. 1194.
(Ae. 356.)

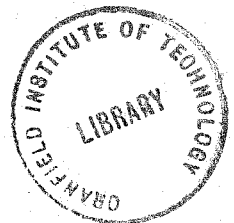
On 10/11/28
A.R.C.
Nat

AN INVESTIGATION OF FLUID FLOW IN TWO
DIMENSIONS.—By A. THOM, D.Sc., Ph.D., A.R.T.C.

Date C
25.5

COMMUNICATED BY
PROFESSOR J. D. CORMACK, C.M.G., C.B.E., D.Sc., M.Inst.C.E.

NOVEMBER 1928.



LONDON:
PRINTED AND PUBLISHED BY HIS MAJESTY'S STATIONERY OFFICE
To be purchased directly from H.M. STATIONERY OFFICE at the following addresses:
Adastral House, Kingsway, London, W.C.2; 120, George Street, Edinburgh;
York Street, Manchester; 1, St. Andrew's Crescent, Cardiff;
15, Donegall Square West, Belfast;
or through any Bookseller.

1929.
Price 1s. 0d. Net.

23-9999

1194
4611

55236

AERODYNAMIC SYMBOLS.

I. GENERAL

- m mass
- t time
- V resultant linear velocity
- Ω resultant angular velocity
- ρ density, σ relative density
- ν kinematic coefficient of viscosity
- R Reynolds number, $R = lV/\nu$ (where l is a suitable linear dimension), to be expressed as a numerical coefficient $\times 10^6$

Normal temperature and pressure for aeronautical work are 15°C . and 760 mm .

For air under these conditions $\left\{ \begin{array}{l} \rho = 0.002378 \text{ slug/cu. ft.} \\ \nu = 1.59 \times 10^{-4} \text{ sq. ft./sec.} \end{array} \right.$

The slug is taken to be 32.2 lb.-mass .

- α angle of incidence
- e angle of downwash
- S area
- c chord
- s semi-span
- A aspect ratio, $A = 4s^2/S$
- L lift, with coefficient $k_L = L/S\rho V^2$
- D drag, with coefficient $k_D = D/S\rho V^2$
- γ gliding angle, $\tan \gamma = D/L$
- L rolling moment, with coefficient $k_L = L/S\rho V^2$
- M pitching moment, with coefficient $k_m = M/cS\rho V^2$
- N yawing moment, with coefficient $k_n = N/s\rho V^2$

2. AIRSCREWS

- n revolutions per second
- D diameter
- J V/nD
- P power
- T thrust, with coefficient $k_T = T/\rho n^2 D^4$
- Q torque, with coefficient $k_Q = Q/\rho n^2 D^5$
- η efficiency, $\eta = TV/P = Jk_T/2\pi k_Q$



AN INVESTIGATION OF FLUID FLOW IN TWO DIMENSIONS.

By A. Thom, D.Sc., Ph.D., A.R.T.C.

Communicated by

Professor J. D. Cormack, C.M.G., C.B.E., D.Sc., M.Inst.C.E.

Reports and Memoranda, No. 1194.

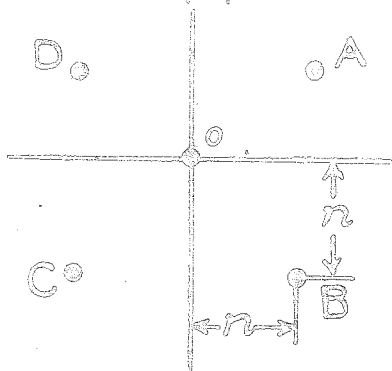
(Ac. 356.)

November, 1928.

PART I.

Flow of an Inviscid Fluid.—There are in existence several methods of obtaining numerical solutions to the two-dimensional flow of a perfect fluid for given boundary conditions. Part 2 of the present paper gives a method of obtaining a numerical solution for viscous steady flow. To form an introduction to the method it is proposed to give another solution of the simpler problem, illustrating it with examples bearing on the experimental work described in Part IV.

Solution of $\nabla^2 \psi = 0$.



In the field of flow consider four points A, B, C and D, placed on the corners of a small square with centre at O and sides equal to $2n$. Let ψ be the value of the stream function at O. Then the values at the corners are by Taylor's Theorem to third order terms.

$$\left. \begin{aligned} \psi_A &= \psi + n \frac{\partial \psi}{\partial x} + n \frac{\partial \psi}{\partial y} + \frac{n^2}{2} \frac{\partial^2 \psi}{\partial x^2} + \frac{n^2}{2} \frac{\partial^2 \psi}{\partial y^2} + n^2 \frac{\partial^2 \psi}{\partial x \partial y} + \\ &\quad \frac{n^3}{6} \frac{\partial^3 \psi}{\partial x^3} + \frac{n^3}{6} \frac{\partial^3 \psi}{\partial y^3} + \frac{n^3}{2} \frac{\partial^3 \psi}{\partial x \partial y^2} + \frac{n^3}{2} \frac{\partial^3 \psi}{\partial x^2 \partial y} \\ \psi_B &= \psi + \quad - \quad + \quad + \quad - \quad + \quad - \quad + \quad - \\ \psi_C &= \psi - \quad - \quad + \quad + \quad + \quad - \quad - \quad - \quad - \\ \psi_D &= \psi - \quad + \quad + \quad + \quad - \quad - \quad + \quad - \quad + \end{aligned} \right\} (1)$$

By adding and dividing by 4, we obtain,

$$\psi = \psi_M - \frac{n^2}{2} \left(\frac{\partial^2 \psi}{\partial x^2} + \frac{\partial^2 \psi}{\partial y^2} \right) \quad \dots \quad \dots \quad \dots \quad (2)$$

where $\psi_M = (\psi_A + \psi_B + \psi_C + \psi_D) \div 4$

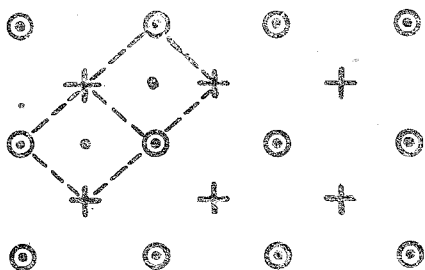
So that when $\nabla^2 \psi = 0$

$$\psi = \psi_M \quad \dots \quad \dots \quad \dots \quad \dots \quad (3)$$

Thus, if we have approximate values of $\psi_A, \psi_B,$ etc., from an assumed field, we can calculate the central value from (3) and this central value will be in general a better approximation than the corner values. Then, we can gradually improve the solution.

Accordingly, the present method of solution is to divide the field into squares and assume values of ψ for each corner. From these calculate the central values and then, using these as the corners of a new set of squares, find new values for the original corners. The process is repeated until the values recur.

Judgment must be exercised in selecting the size of square. It will be noticed that the method is correct to third order quantities but not to fourth (as may be seen by writing the next terms in Taylor's Theorem). As the approximations get closer, the squares should be reduced in size. They are easily halved by interpolating values (using (3)) in the diamond squares, that is those squares which are formed with their diagonals vertical as shown dotted in the figure annexed.



In practice, a difficulty arises when the squares at the edge of the field cannot be arranged with their outer corners on the boundary; but this is easily overcome by interpolating the values (graphically or otherwise) or by breaking up the region into smaller squares.

As an illustration of the method, the field chosen is that produced by the solid whose trace is two infinite parallel straight lines joined by a semicircle (see Fig. 1). The nearest approach to a theoretical solution known to the author for these boundaries is that by W. M. Page* the difference being that there the lines are joined by a cycloid.

Two cases were worked :—

- (a) Fluid infinite.
- (b) Fluid bounded by a plane at a distance of 8 radii.

* "Some two dimensional problems in electrostatics and hydrodynamics".
 Proc. Lon. Math. Soc. 1912-13, page 323.

Case (a) was somewhat laborious to solve as it meant working over and over an ever increasing number of squares of increasing size until no change was produced in the neighbourhood of the semicircle. Actually, the process was stopped at 80 radii. The streamlines obtained are shown for the inner part of the field in Fig. 1.

The pressures round the semicircle or rather semicylinder are easily obtained and are shown plotted in Fig. 2. The resemblance to the experimental pressures on the front half of a cylinder at high values of VD/v is obvious.

Case (b) was much easier, having a definite boundary above. The streamlines differ but little from Fig. 1 and the pressures are shown in Fig. 2. Further use will be made of these fields in the appendix.

After the above work was completed Dr. Hague drew the writer's attention to a paper by A. O. Müller* in which the above solution of $\nabla^2 \psi = 0$ is discussed and ascribed to Liebmann†.

PART II.

Viscous Flow.—The general equations of two-dimensional motion of a viscous fluid are

$$\left. \begin{aligned} X - \frac{1}{\rho} \frac{\partial p}{\partial x} &= \frac{\partial u}{\partial t} - \nu \nabla^2 u + u \frac{\partial u}{\partial x} + v \frac{\partial u}{\partial y} \\ Y - \frac{1}{\rho} \frac{\partial p}{\partial y} &= \frac{\partial v}{\partial t} - \nu \nabla^2 v + u \frac{\partial v}{\partial x} + v \frac{\partial v}{\partial y} \end{aligned} \right\} \dots \quad (4)$$

If the motion is steady and no external forces are acting

$$\frac{\partial u}{\partial t} = \frac{\partial v}{\partial t} = X = Y = 0$$

An alternative form for these equations in which p has been eliminated is

$$\nu \nabla^2 \zeta = u \frac{\partial \zeta}{\partial x} + v \frac{\partial \zeta}{\partial y} \quad \dots \quad (5)$$

We also have

$$u = - \frac{\partial \psi}{\partial y}, \quad v = \frac{\partial \psi}{\partial x}, \quad \nabla^2 \psi = 2 \zeta \dagger \quad \dots \quad (6)$$

* "Über eine neue Methode zur Zeichnung der Feldbilder magnetischer Kraftlinien". Archiv für Elektrotechnik, vol. XVII, p. 501, 1926.

† "Verfahren zur numerischen Lösung partieller Differentialgleichungen zweiter Ordnung", Sitzungsberichte der Bayerischen Akademie der Wissenschaften, 1918.

‡ In Lamb's "Hydrodynamics" $\nabla^2 \psi = \zeta$ but the form given above is retained here.

As in Part I, consider a square in the field. The relation deduced there for ψ (Equation 2) is quite general so that we have for the values of ψ and ζ at the centre of the square.

$$\psi = \psi_M - \frac{1}{2} n^2 \nabla^2 \psi \dots \dots \dots (7)$$

$$\zeta = \zeta_M - \frac{1}{2} n^2 \nabla^2 \zeta \dots \dots \dots (8)$$

Neglecting third order quantities suitable combinations of Equations 1 give.

$$\left. \begin{aligned} \partial\psi/\partial x &= (A+B - C - D) \div 4n \\ \partial\psi/\partial y &= (A+D - B - C) \div 4n \\ \partial\zeta/\partial x &= (a+b - c - d) \div 4n \\ \partial\zeta/\partial y &= (a+d - b - c) \div 4n \end{aligned} \right\} \dots (9)$$

where $A = \psi_A, a = \zeta_A, B = \psi_B, b = \zeta_B$, etc.

Then from (5), (8) and (9) we get

$$\zeta = \zeta_M - \frac{1}{16v} \left\{ (a-c)(B-D) + (b-d)(C-A) \right\} (10)$$

and from (6) and (7)

$$\psi = \psi_M - n^2 \zeta \dots \dots \dots (11)$$

These are the expressions to be used in improving an assumed field in viscous flow as (3) was used for the perfect fluid, the difference being that we must now start with assumed values of ζ as well as of ψ .

In many cases the values of ψ is known along the boundaries* but this is not so with the vorticity and it is necessary to use some additional method for obtaining the approximation to ζ on the surface where the fluid flows over a solid. Consider a small portion of the surface. For the moment take the axis of x along, and the axis of y normal to the surface. As a first approximation write

$$\zeta = \zeta_0 + ky \dots \dots \dots (12)$$

If y is small the normal velocity $v = \partial\psi/\partial x$ will be small throughout the region. Hence, approximately $\partial^2\psi/\partial x^2 = 0$ so that $2\zeta = \partial^2\psi/\partial y^2$

Hence

$$\frac{\partial^2\psi}{\partial y^2} = 2\zeta_0 + 2ky$$

Integrating twice and assuming that ψ is zero on the surface, we get

$$\psi = \zeta_0 y^2 + \frac{1}{3} ky^3 \dots \dots \dots (13)$$

* Care should be taken in applying the method where the boundaries form a definite angle as the continuity has been assumed in deducing these formulæ.

Let ψ_1 and ψ_2 be the values of ψ when y is y_1 , and y_2 respectively. Substituting these values in (13) and eliminating k leads to

$$\zeta_0 = \frac{y_2^3 \psi_1 - y_1^3 \psi_2}{y_1^2 y_2^2 (y_2 - y_1)} \quad \dots \quad \dots \quad \dots \quad (14)$$

This gives the required value of the surface vorticity in terms of two values of ψ near the surface. If it is legitimate to put $k = 0$, i.e., to assume ζ constant throughout the neighbourhood, we have the simpler expression

$$\zeta_0 = \psi_1 / y_1^2 \quad \dots \quad \dots \quad \dots \quad \dots \quad (15)$$

If on the other hand it is considered necessary to take into account the variation of ψ with x it can be done as follows:—By Taylor's Theorem put

$$\psi = ay + bx + cy^2 + dx^2 + exy + fy^3 + gx^3 + hx^2y + iy^2x$$

where $a = \partial\psi/\partial y$, etc., as in (1).

If $y = 0$ we have by differentiation

$$\partial\psi/\partial x = b + 2dx + 3gx^2$$

but $\partial\psi/\partial x = v$ and hence is zero for all values of x .

$$\therefore b = d = g = 0$$

similarly by differentiating with respect to y we get

$$a = e = h = 0$$

So the approximate expression for ψ near the boundary is

$$\psi = cy^2 + fy^3 + iy^2x$$

The coefficient c is the value of $\frac{1}{2} \frac{\partial^2\psi}{\partial y^2}$ when $y = 0$, but we have already seen that this is equal to ζ_0 . So to determine ζ_0 take three points in the field (x_1y_1) , (x_2y_2) , and (x_3y_3) and note the corresponding values of the stream function ψ_1 , ψ_2 and ψ_3 . This gives three equations to solve for c or ζ_0 . Algebraically the solution is found to be

$$\zeta_0 = \frac{\frac{\psi_1}{y_1^2}(y_2x_3 - y_3x_2) + \frac{\psi_2}{y_2^2}(y_3x_1 - y_1x_3) + \frac{\psi_3}{y_3^2}(y_1x_2 - y_2x_1)}{y_1(x_2 - x_3) + y_2(x_3 - x_1) + y_3(x_1 - x_2)} \quad (16)$$

Every time a new set of values of ψ and ζ have been found throughout the field (by 10 and 11) it is necessary to find new values of ζ_0 along the solid boundaries by 14, 15, and/or 16.

The whole process must be repeated until the values of ψ and ζ recur to within what is considered a satisfactory margin throughout the field. This margin must be only a fraction (say 1/10) of the accuracy required in the solution as the quantities only approach their limit slowly. The field can now be plotted and the velocities

obtained, but if pressures are required a further step is necessary. This step (which consists of integrating certain quantities along chosen lines in the field) is desirable as it can be made to give a check on the solution.

Taking the second equation of (4), we have

$$-\frac{1}{\rho} \frac{\partial p}{\partial y} = -v \nabla^2 v + u \frac{\partial v}{\partial x} + v \frac{\partial v}{\partial y}$$

but $\nabla^2 v = \frac{\partial^3 \psi}{\partial x^3} + \frac{\partial^3 \psi}{\partial x \partial y^2} = 2 \frac{\partial \zeta}{\partial x}$

hence $-\frac{1}{\rho} \frac{\partial p}{\partial y} = -2v \frac{\partial \zeta}{\partial x} + v \frac{\partial v}{\partial y} + u \frac{\partial u}{\partial y} + 2u\zeta$

Integrating between A and B (two points on the line $x = \text{const}$) we get

$$p_A + \frac{1}{2} \rho q_A^2 = p_B + \frac{1}{2} \rho q_B^2 - 2 \rho v \int_A^B \frac{\partial \zeta}{\partial x} dy + 2 \rho \int_A^B u \zeta dy \dots (17)$$

where $q^2 = u^2 + v^2$

Similarly from the first equation of (4) we get for two points on $y = \text{const}$.

$$p_A + \frac{1}{2} \rho q_A^2 = p_B + \frac{1}{2} \rho q_B^2 + 2 \rho v \int_A^B \frac{\partial \zeta}{\partial y} dx - 2 \rho \int_A^B v \zeta dx \dots (18)$$

The last two terms of these expressions therefore give the change of total head between A and B. So that knowing the total head at a point C it can be found at any other point D by joining C and D by a path consisting of straight lines parallel to the x or y axis and integrating the above expressions graphically along the lines. If the path is closed a severe check is obviously obtained on the part of the field traversed by the path.

PART III.

Viscous Flow past a Circular Cylinder at $R = 10$.—The method developed in Part II has been used to form the solution of the equations of steady viscous flow past a cylinder between parallel walls 8 diameters apart. To simplify the arithmetic as far as possible the following values were adopted.

- Velocity of undisturbed flow = $V = 6.25$ units/sec.
- Coefficient of kinematic viscosity = $\nu = 6.25$
- Radius of Cylinder = 5 units
- Distance between walls = 80 units
- Reynolds Number = $R = VD/\nu = 10$

Since the vorticity was assumed to be zero along the straight boundary walls the solution developed is really that past a series of

cylinders at distance apart 80 units or 8 diameters. The circle of radius 5 passes through the corners of 12 squares of side unity, thus simplifying the work. With the above values we get from 10 and 11

$$\zeta = \zeta_M - 0.01n^2 \{ (a - c) (B - D) + (b - d) (C - A) \}$$

$$\psi = \psi_M - n^2 \zeta$$

To begin the solution a field was assumed by calculating values from the expressions for the flow of an infinite inviscid fluid past a cylinder of radius 20 per cent. greater than the actual cylinder to allow for the retardation over the surface. This was corrected to suit the straight boundary by the method given in Part I. The inner part was then "faired" to the cylinder, the surface values of ζ on the front portion being estimated from the boundary layer solution in R. & M. 1176. The assumed field was symmetrical in front and behind (i.e., about the y axis).

The expressions given above were then applied to the field over and over again in conjunction with 14, 15 and 16. The field soon lost its symmetry. The process was laborious, the more so as it had to extend from about 5 diameters up stream to 8 down stream. In all about 1,600 numerical substitutions were made in 10 and 11. As the work proceeded short cuts suggested themselves, such as extrapolating the next values from the run of the figures. The solution obtained could certainly be improved, but some regions would then require the use of smaller squares which would add enormously to the work.

A portion of the work near the cylinder is shown in Fig. 3. At greater distances larger squares were of course permissible. The key given explains the figures which show the degree of approximation obtained. Near the cylinder surface the squares were afterwards reduced as in Part I and in places again reduced, but this work is not shown. The outer parts of the field are given in skeleton in Table 1. Figs. 4 and 5 show the streamlines and vorticity contours near the cylinder. Along the line $x = 10$ the vorticity is practically zero so that at this section the total head is that in the undisturbed stream. Hence, integrating 18 along $y = 0, y = 3, y = 4$ and $y = 5$ from this section to the surface gives pressures on the surface. The pressures behind the cylinder were got by integrating along $y = 6$ and then along $x = 0, x = -3, x = -4, x = -5$ from the line $y = 6$ to the surface. Several points were checked by integrating right through the vorticity region from above. The results are

θ	$p_1 = \frac{p - p_0}{\frac{1}{2} \rho V^2}$
0°	1.43
37	+0.67
53	-0.4
90	-1.5
127	-1.6
143	-1.4
180	-1.3

From these the coefficient of normal pressure drag is easily deduced and found to be 0.95.

It remains to find the viscous or skin friction drag. From Lamb's Hydrodynamics we have

$$p_{xy} = \mu \left(\frac{\partial v}{\partial x} + \frac{\partial u}{\partial y} \right)$$

Taking for the moment x along the surface, this reduces to $p_{xy} = \mu \frac{\partial u}{\partial y}$ where p_{xy} is now the tangential force,

but
$$2\zeta_0 = \frac{\partial v}{\partial x} - \frac{\partial u}{\partial y} = - \frac{\partial u}{\partial y} \text{ since } \frac{\partial v}{\partial x} = 0$$

$$\therefore p_{xy} = - 2\mu \zeta_0$$

This can be integrated to give the viscous drag and expressed as a coefficient is found to be for the present example 0.74. Hence, the total drag coefficient found for a cylinder at $R = 10$ is $0.95 + 0.74 =$ say 1.7. The experimental value as found by E. F. Relf (R. & M. 102) is about 1.6 which is certainly a closer agreement than was to be expected considering that the solution above has hardly been carried far enough.

PART IV.

Experimental Determination of the Pressures round a Stationary Cylinder in an Air Current throughout a large Range of Reynolds Number.

Many determinations of the pressure distribution round a circular cylinder have been made in various laboratories but these have mostly been at relatively high values of Reynolds Number.

The theory of the subject has only been developed for very low scale values ($R < 10$) if we except those theories which seek to reproduce the actual conditions by placing eddies behind the cylinder in positions partly determined by theory and partly by experiment (Kármán, Levy, etc.). Presumably, the theory will gradually be completed for higher values of R so that it seems desirable to find experimentally the pressure distribution for as large a range as possible.

The present set of experiments cover the range between $R = 28$ and $R = 17,000$ the lower values being of less accuracy than the others. For each experiment the drag due to the normal pressure has been obtained by integration. At the lower values of R the viscous surface drag becomes relatively large as is shown by comparison of these results with the total drag determined by E. F. Relf.

A bye-product of these experiments has been a determination of the effect of the size of the hole pierced in the surface. Three sizes of cylinder were used, namely, $7/8"$, $1/8"$ and $1/40"$ diameter. The first two stretched right across the channel and the last was long, compared with its diameter, so that the flow was assumed two-dimensional in all cases.

At the lower velocities 2-5 ft./sec., a close mesh wire gauze was placed over the mouth of the channel. While this certainly helps to produce an even flow its primary object was to increase the sensitiveness of the pressure gauge to velocity changes, one side of this gauge being connected to a flush plate inside the channel and the other open to the atmosphere. The head lost in the gauze is thus included in the gauge reading so that even at 2 ft./sec. a reasonable movement is obtained. This gauge was used to enable the channel speed to be adjusted to the same value during each position of the hole in the cylinder. The actual channel speed was deduced from the observations themselves.

Special attention was directed to ensuring that the results could be referred to the true static pressure. This problem is bound up with the question of the interference of the channel walls which is discussed in Appendix 1. A long brass tube $1/8"$ diameter was suspended along the channel centre line. A group of small holes was drilled in this tube at the section to be afterwards occupied by the cylinder. The pressure in these holes was then compared with that in two static plates A and B. Plate A was flush with the channel floor, the hole being directly under the cylinder position. Plate B was about 3 ft. up channel where the pressure would be unaffected by the presence of the cylinder. These comparisons were made at all speeds with the gauze on and off. The static tube was then removed and a comparison made between plate A and plate B. This was repeated with two different cylinders in position. It was found that the presence of the cylinder caused a fall of static pressure at plate A. This is due to two causes.

(a) If there were no channel walls restricting the flow there would still be an increase of speed past the cylinder and hence a drop of pressure.

(b) The presence of the channel walls by "compressing" the streamlines causes a further increase of velocity. In order to reduce the results approximately to the condition of free flow, it is necessary to separate these two effects. For the $7/8"$ diameter cylinder the correction is small and the consideration of it is given in Appendix 1. For the smaller cylinders it is obviously quite negligible.

For the actual pressure determinations a tilting gauge was connected between plate A and the hole in the cylinder. To eliminate the effects of creep in the velocity and pressure gauges the pressure on the front generator (which, after correction is assumed to be $\frac{1}{2}\rho V^2$) was read after every fourth or fifth reading and the individual

readings in each group were as far as possible distributed round the circumference. As the readings are carried right round the cylinder any constant error in θ is eliminated when means are taken.

The small cylinder (diameter 1/40") presented a set of difficulties on its own. The greatest of these was the throttling effect of the necessarily small hole and passage. This was partly got over by drilling three holes in line along a generator, but even then there remained the constricted passage through the cylinder itself and slight changes of temperature caused large fluctuations in the gauge pressures. A hand held near the cup of the gauge caused a rise in pressure due to the fact that the expanded air did not get away freely. It was quite impossible to work on windy days, a flat calm being necessary. Every gust of wind outside the building caused fluctuations in pressure of the order of the total difference being measured at the lower speeds. Opening or closing of doors in other parts of the building was particularly objectionable. When it is recalled that at 2 ft./sec. $\frac{1}{2}\rho V^2$ is equivalent to a head of water of about 0.001 inch, the difficulties will be apparent. In fact the style of manometer used is no longer suitable. Nevertheless, the results obtained at this speed are given for what they are worth. A further complication arises from the fact that the pressure on the front generator of the small cylinder at low speeds is no longer $\frac{1}{2}\rho V^2$. For this reason a small pitot tube was placed in the channel about 10 cm. above the small cylinder and the pressure in this tube measured after each group in the same way as the front generator pressure was measured for the larger cylinders.

In addition the pressure on the front generator of the small cylinder was compared with this pitot for a range of wind-speeds between 2 and 10 ft./sec. These results are given in Table 2, p' being the observed pressure difference between the cylinder and the pitot.

Table 3 gives the results of the pressure determination for all three cylinders. These pressures have been corrected where necessary as already indicated so that they refer to the static pressure in undisturbed free flow.

Size of Hole.—Four different sizes of hole were used in the 7/8" diameter cylinder and two in the 1/8". An analysis of these results showed that for each cylinder, they can be brought into substantial agreement if it is assumed that the pressure inside the cylinder is, not the pressure at the centre of the hole in the surface, but that at a point half way along the hole radius towards the front of the cylinder. In other words, if θ_0 is the angle between the front generator and the centre of the hole, then the measured pressure corresponds to $\theta = \theta_0 - \frac{1}{2}d/D$ where d = hole diameter, and D = cylinder diameter. This correction has been applied to all the results in Table 3. The plotted results for the 7/8" cylinder (Fig. 6) seems to be sufficient justification for this proceeding. It is rather surprising to note how even the results obtained with a $\frac{1}{4}$ " hole are brought into agreement

with those from a 1/64" hole. These remarks apply to the front portion of the cylinder. Behind, where the pressure gradient is small, the correction naturally makes little difference. For the short region where the pressure is rising rapidly the evidence is inconclusive.

The above results have been brought together in Figs. 7 and 8 along with others from various sources. The pressure coefficient p_1 is a function of θ and R and so is shown by contours in Fig. 8. The sources of information for the various parts of the diagram are given by the reference letters down the right side and are as follows:—

- A. Present report (Part IV) Experimental.
- B. Present report (Part III) Theoretical.
- C. R. & M. No. 1176. Corrected.
- D. Fage, Communicated. (See R. & M. No. 1179).
- E. Fage, Communicated. (Unpublished).
- F. Fage, R. & M. No. 106.
- G. Taylor, R. & M. No. 191.
- H. Parkin, R.A.S. Journal, No. 204, Vol. XXXI.
- I. Lamb, Hydrodynamics.

In dealing with published experiments it has been assumed (in the absence of a statement to the contrary) that the pressures have not been previously corrected for the "compression" introduced by the channel walls. This correction has been applied assuming the velocity increment to be $v_1/V = 13 \div (30r + r^2)$ where r is the ratio of channel depth to cylinder diameter. (See Appendix.) The resultant correction to the individual values of p_1 is $2 v_1/V (1 - p_1)$ approximately.

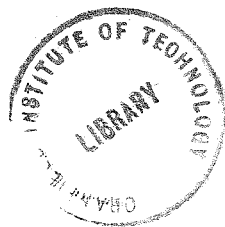
This correction becomes considerable in the case of experiments such as those of A. Fage with a cylinder 8.9" diameter in a 4 ft. channel which of course were not intended for the present purpose but reached a higher value of R than any other known to the writer.

Coming to the other end of the scale we have Lamb's solution for low values of R. Adopting the notation and convention of this report the expression for the pressure at the cylinder surface is found to be:—

$$p_1 = \frac{1 - 2 \sin^2 \theta - \frac{8}{R} \sin \theta}{\frac{1}{2} - \gamma - \log \frac{R}{8}}$$

It has been assumed that this solution is valid up to $R = 0.4$. From here to $R = 25$ Bairstow's solution would be appropriate but it does not seem to be possible to get the pressure distribution from it without additional mathematical investigation as the authors state that they neglect a constant term* which does not affect the total

* "The resistance of a cylinder moving in a viscous fluid". L. Bairstow, Cave and Lang. Phil. Tr. A. Vol. 223, p. 402.



resistance but would presumably affect the individual pressures. As no information is available in this region the contours on Fig. 8 have been dotted in by inspection and of course cannot be relied on.

Drag.—The drag produced by the normal pressure has been calculated from the experimental pressures given in Table 3. The results are given in the form of a coefficient $K'_D = \text{Drag} \div \rho DLV^2$ in Table 4. Fig. 9 shows the values plotted on $\log_{10} R$. The total drag coefficient as determined by E. F. Relf by force measurements is also shown. The difference between the two is the skin friction drag and is shown chain dotted.

In R. & M. No. 1176 it is estimated that the skin friction drag is equal to $2/\sqrt{R}$ and this value is also plotted in Fig. 9 showing a reasonable agreement with the above. The values obtained by the arithmetical solution of the fundamental equations in Part III are also shown and used to produce the curves.

APPENDIX.

Effect of the Channel Walls on the Flow past a Cylinder.

The presence of parallel channel walls above and below a horizontal cylinder by preventing the expansion or bulge of the streamlines increases the mean velocity past the cylinder. An estimate of this increase has been made in R. & M. No. 1018 by considering the flow of an inviscid fluid past a rotating cylinder. If r is the ratio of channel height to cylinder diameter then the mean increase in velocity is there estimated to be about $100/r^2$ per cent. This value seems to be too low for a stationary cylinder. This is probably due to the eddying region behind the cylinder preventing the streamlines from closing for some distance. It is evident that this will produce a larger "bulge" at the cylinder. This is shown by the field obtained in Part I for the flow past the solid shown in Fig. 1. The "bulge" of the streamlines at various distances across the section of this field through the centre of the semi-circular arc is shown in Fig. 10. When two parallel boundaries were placed at distances of 8 radii from the axis and the solution repeated the increment in velocity at various points across this section was found to be about 7 per cent. agreeing with that given in Fig. 10. This figure also shows the "bulge" given by the expression obtained by Levy for the flow past a cylinder with a vortex pair behind it.*

To obtain further experimental information the decrement in pressure on the channel wall exactly below the centre of the cylinder due to the presence of the latter was measured with the following results.

Cylinder diameter in.	r	$\Delta p / \frac{1}{2} \rho V^2$ Pressure decrement per cent.	v_3/V Velocity increment per cent.	From Field in Fig. 1.		
				v_2/V per cent.	v_1/V per cent.	$v_3/V = (v_1 + v_2)/V$ per cent.
0.875	30	3	1.5	0.7	1.1	1.8
3.15	8.2	16	8	1.0	6.0	7.0

This velocity increment may be divided into two parts v_1 and v_2 arising from different causes. The first v_2 is the increase in velocity which would have existed at this point had there been no channel walls at all and the second v_1 is that produced by the compression of the flow produced by the walls. The last three columns give the values computed from the field which is shown in Fig. 1. In plotting these values in Fig. 10 it has been assumed that $v_1 = v_2$ so that the plotted value is $\frac{1}{2} v_3/V$.

When the pressure distribution has been measured on a large cylinder in a small channel and the true drag coefficient for the cylinder at this R is known, we can deduce a value for the correction to the mean velocity. Such a case is that given in R. & M. 1176. J. H. Parkin in Toronto has also carried out a series of experiments on channel wall interference for cylinders of various lengths, etc. His results for the cylinder spanning the channel are also shown in Fig. 10.

After considering the somewhat inconsistent evidence available it was decided to adopt the following provisional value for the correction.

$$\frac{v_1}{V} = \frac{13}{30r + r^2} \text{ for } r \leq 5$$

* Aeronautical Journal. Vol. XXIII., p. 326.

For a cylindrical body of any cross section provided the dimension in the direction of the flow is small compared to the height of the channel v_1 is nearly equal to v_2 . This can be seen by replacing the channel walls by images of the body. The effect of the nearest image on one side will be to give an additional velocity increment v_2 and at the same time a similar increment is being produced on the other side. So that the average increment given by the channel walls is of the same magnitude as that existing at the position of the channel walls if these were removed. Thus, either of these increments is half the total as obtained in the channel by the above method of measuring the pressure increment on the wall opposite the section. For a body like an aerofoil which has a small wake, this should give a fairly reliable method of measuring the compression correction provided the body spans the channel. For a body with a section long in the direction of flow (such as that in Fig. 1) v_1 will be greater than v_2 .

TABLE 1.

Skeleton Solution for Viscous Flow Past a Cylinder.

Upper figures are values of ζ .

Lower figures are values of ψ .

$\begin{array}{c} x \\ \rightarrow \\ \swarrow \\ y \\ \downarrow \end{array}$	-41	-33	-25	-17	-9	-1	+7	+15	+23	+31	+ α
40	0 250	0 250	0 250	0 250	0 250	0 250	0 250	0 250	0 250	0 250	0 250
32	0.01 184	0 183	0 183	0 184	0 187	0 189.9	0 193.1	0 194.8	0 198.0	0 199.0	0 200
24	0.06 120	0.08 117	0.05 116	0.03 117	0 122	0 129.6	0 136.1	0 142.0	0 146.3	0 148.3	0 150
16	0.12 65	0.14 60	0.16 56	0.19 54.6	0.15 58.4	0.02 67.5	0 79.7	0 89.6	0 95.4	0 98.0	0 100
8	0.13 26	0.14 21.5	0.18 16.6	0.27 12.7	0.38 9.6	0.78 9.1	0.06 28.0	0 41.2	0 46.8	0 48.7	0 50
0	0 0	0 0	0 0	0 0	0 0		0 0	0 0	0 0	0 0	0 0

TABLE 2.
 Pressure on Front Generator of Small Cylinder.

V ft /sec.	p' lb./ft. ²	$\frac{p - p_0}{\frac{1}{2}\rho V^2}$
1.9	0.021	1.5
3.1	0.020	1.18
4.4	0.028	1.12
5.6	0.027	1.07
8.4	0.017	1.02
10.6	0.021	1.016

p = pressure on front generator.

p_1 = pressure in pitot.

$p' = p - p_1$ (observed).

p_0 = static pressure in the undisturbed flow.

Cylinder diameter = 0.66mm.

TABLE 3.—continued.

Common to all.	D = 3.2		D = 3.2		D = 22.2		D = 22.2		D = 22.2		D = 22.2		D = 22.2		
	d	p_1	d	p_1	d	p_1	d	p_1	d	p_1	d	p_1	d	p_1	
0	1.00	0	1.00	0	1.000	0	1.000	0	1.000	0	1.000	0	1.000	0	1.00
10	0.96	9	0.92	9	0.905	8.7	0.941	5.8	0.965	2	0.983	2	0.983	0	0.91
20	0.76	19	0.68	19	0.650	18.7	0.684	15.8	0.764	12	0.83	12	0.83	9.5	0.65
30	+0.38	29	+0.30	29	29.5+0.235	28.7+0.293	25.8+0.388	25.8+0.388	22	22	0.50	22	0.50	19.5	0.65
40	-0.05	39	-0.17	39	39.5-0.265	38.7-0.198	35.8-0.098	35.8-0.098	32	32	+0.04	32	+0.04	19.5	+0.23
50	-0.51	49	-0.61	49	49.5-0.56	48.7-0.718	45.8-0.603	45.8-0.603	42	42	-0.45	42	-0.45	39.5	-0.25
60	-0.88	59	-0.96	59	59.5-1.130	58.7-1.058	55.8-1.010	55.8-1.010	52	52	-0.90	52	-0.90	49.5	-0.75
70	-1.09	69	-1.10	69	69.5-1.297	68.7-1.311	65.8-1.255	65.8-1.255	62	62	-1.27	62	-1.27	59.5	-1.13
80	-1.04	79	-1.03	79	79.5-1.204	78.7-1.166	75.8-1.240	75.8-1.240	72	72	-1.39	72	-1.39	69.5	-1.30
90	-0.88	89	-0.90	89	89.5-0.76	88.7-0.71	85.8-1.041	85.8-1.041	82	82	-1.08	82	-1.08	79.5	-1.16
100	-0.82	99	-0.83	99	89.5-0.71	89.5-0.71	86.8-1.019	86.8-1.019	82	82	-1.02	82	-1.02	89.5	-1.07
120	-0.80	119	-0.80	119	119.5-0.72	118.7-0.72	115.8-1.020	115.8-1.020	112	112	-1.07	112	-1.07	99.5	-1.06
140	-0.80	139	-0.82	139	139.5-0.68	138.7-0.68	135.8-1.076	135.8-1.076	132	132	-1.07	132	-1.07	119.5	-1.09
160	-0.80	159	-0.82	159	159.5-0.71	158.7-0.71	155.8-1.094	155.8-1.094	152	152	-1.11	152	-1.11	139.5	-1.15
180	-0.80	180	-0.81	180	180.0-0.70	180.0-0.70	180.0-1.115	180.0-1.115	180	180	-1.05	180	-1.05	159.5	-1.18
															180.0-1.23

(36008)

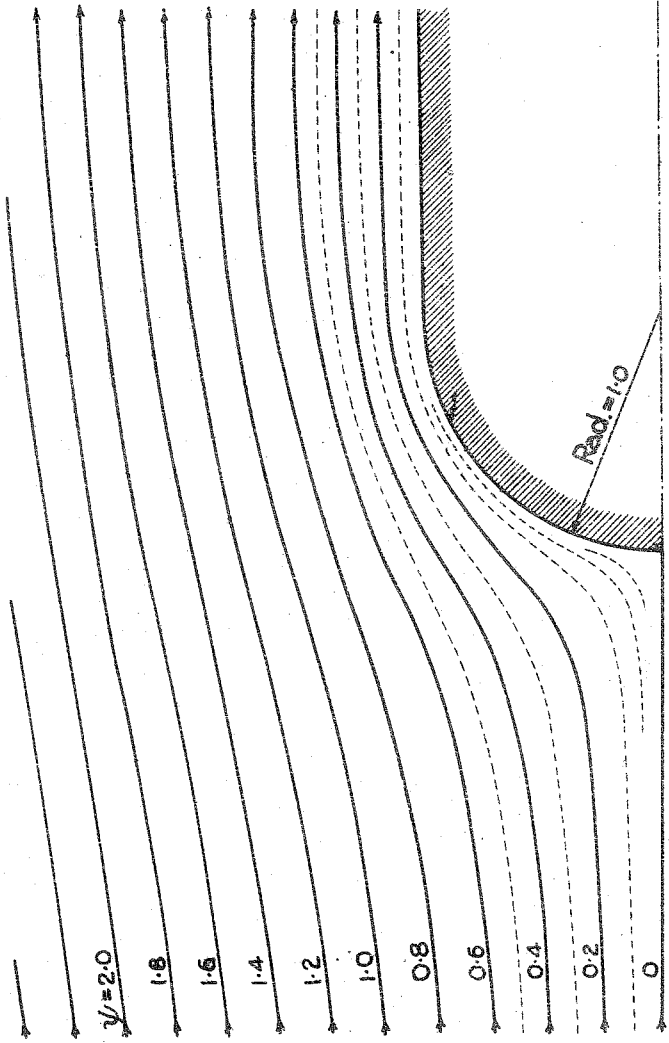
B

TABLE 4.

Cylinder diameter.	Wind speed.	VD/ν	Normal pressure Drag Coefficient.
mm.	ft./sec.		
0.66	2.1	28	0.51
0.66	5.2	70	0.44
0.66	18.6	250	0.50
0.66	35.7	484	0.47
3.2	2.2	144	0.52
3.2	5.5	360	0.48
3.2	18.5	1,240	0.438
3.2	39.2	2,500	0.456
22.2	6.3	2,900	0.43
22.2	18.6	8,500	0.561
22.2	37.3	17,000	0.600

R. & M. 1194.

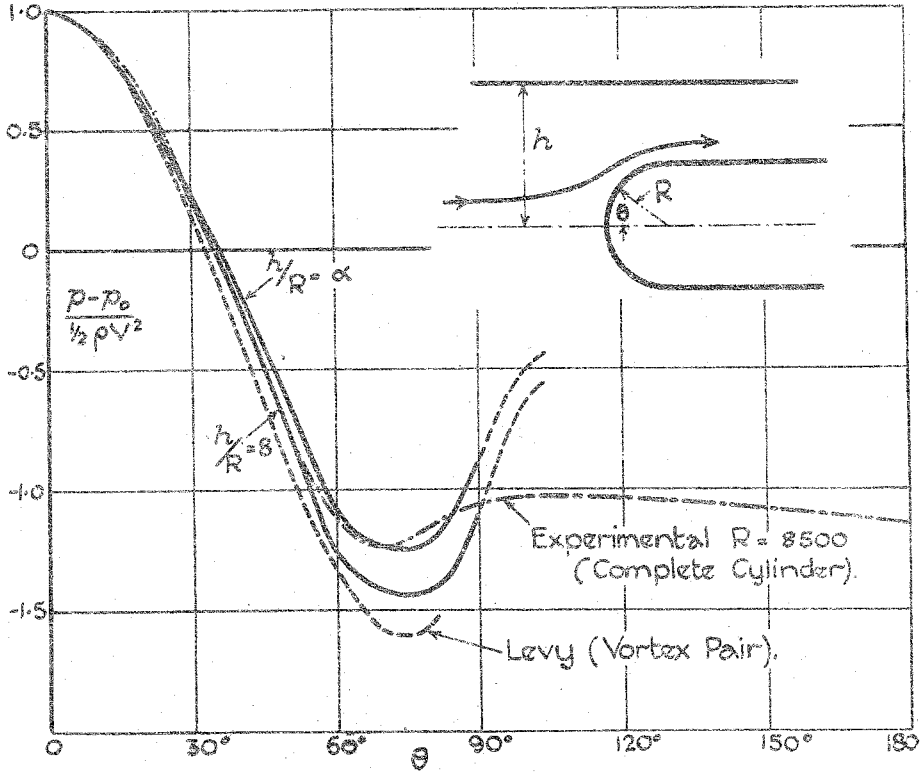
FIG. 1.



R & M. 1194.

FIG. 2.

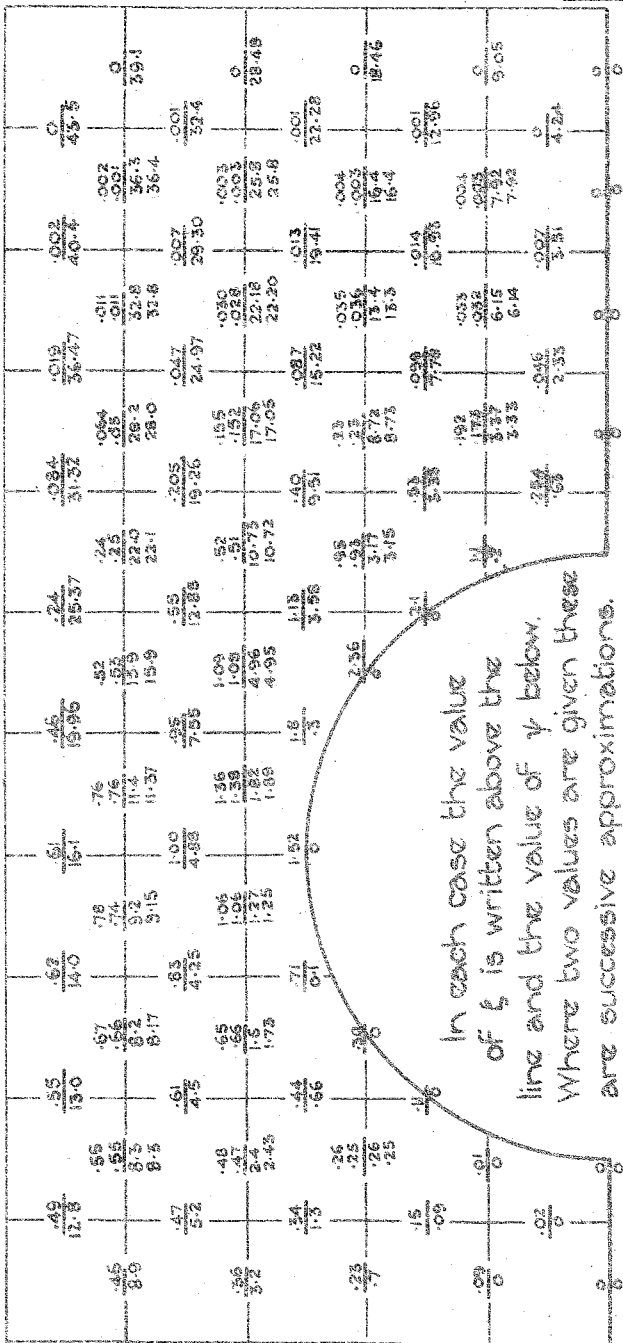
Pressures as obtained by Theory
for Perfect Fluid.



R. & M. 1194.

Final Values in the Numerical Solution of the Viscous Flow
past a Cylinder:

Inner Part of Field.

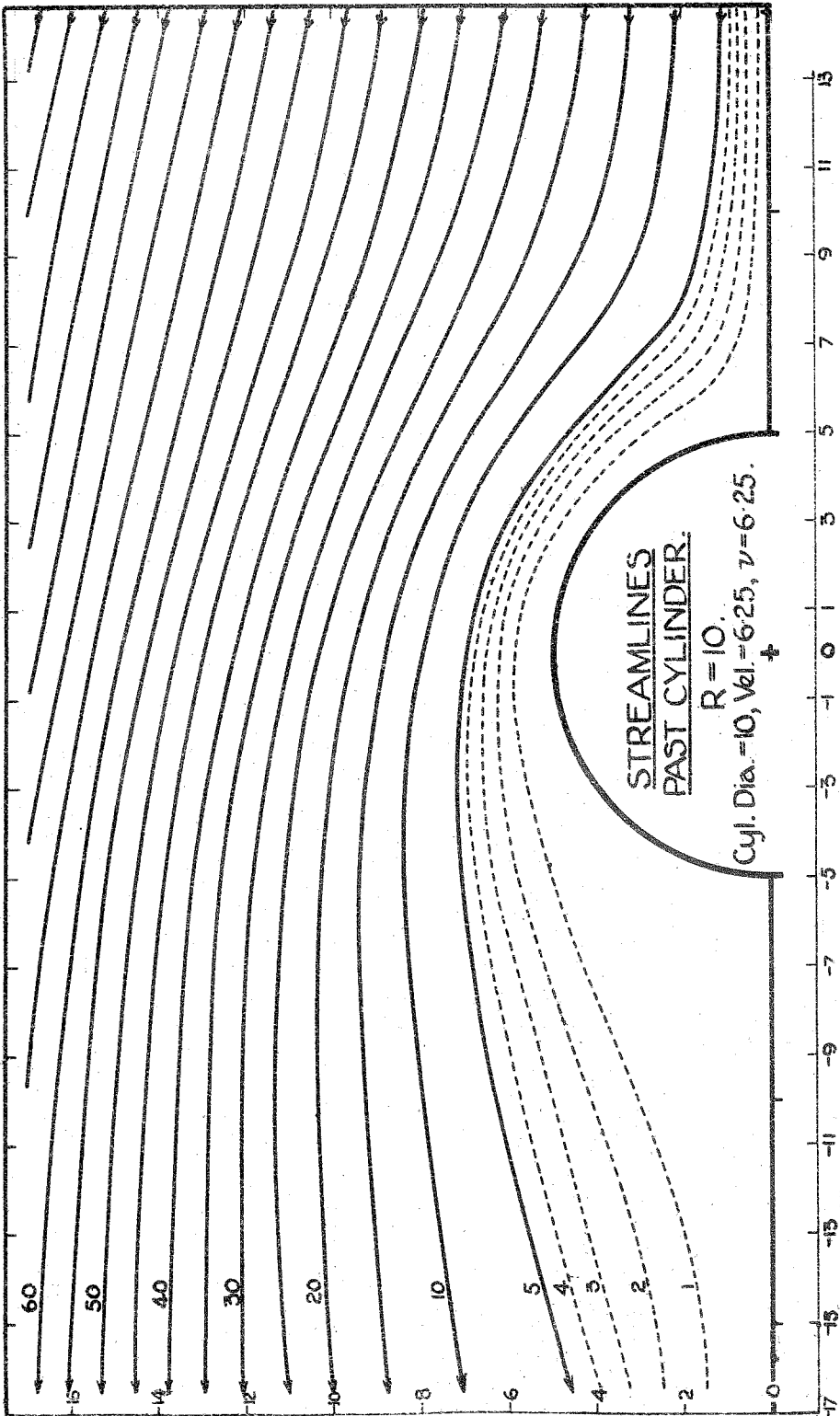


In each case the value
 of ξ is written above the
 line and the value of η below.
 Where two values are given these
 are successive approximations.

FIG. 3.

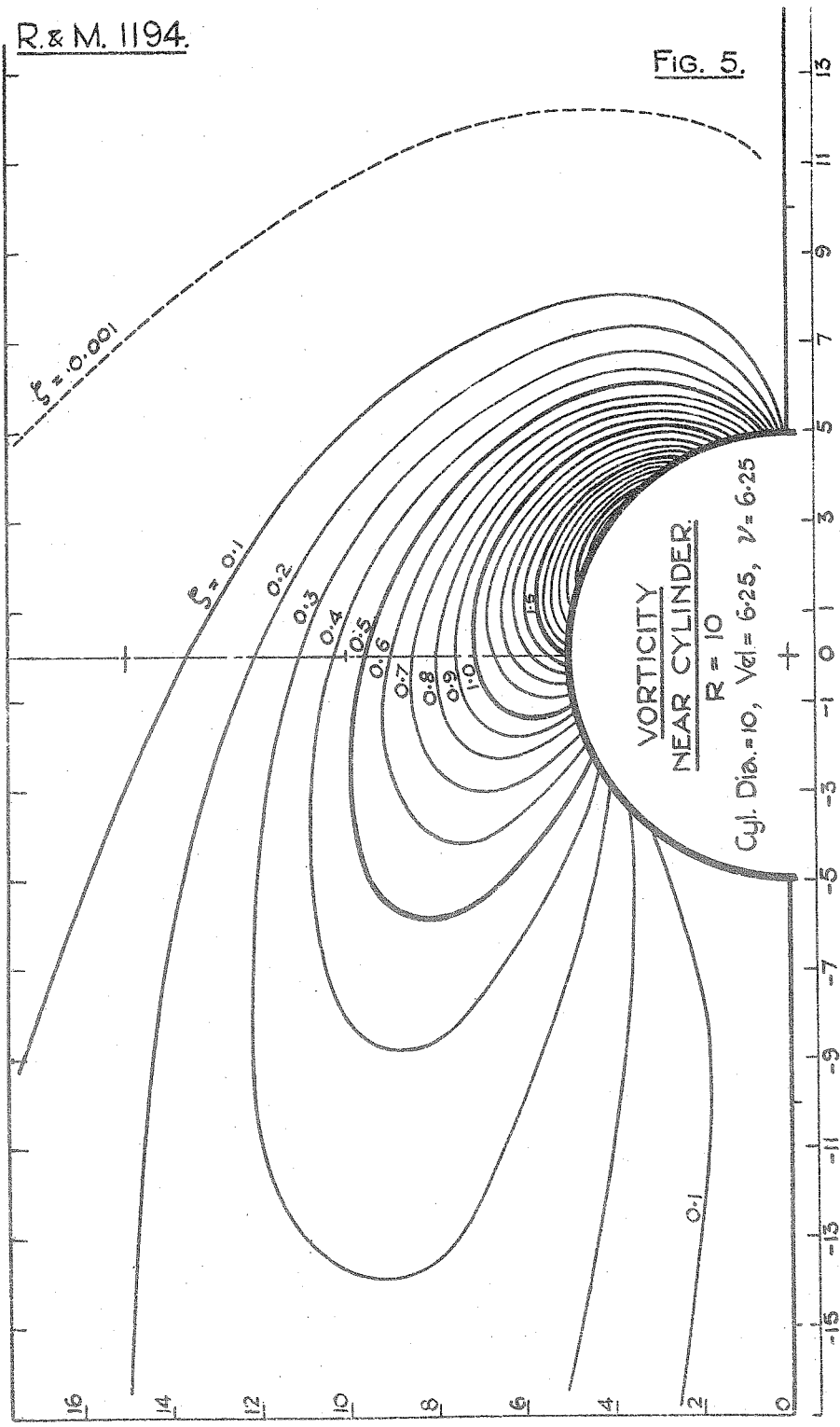
R & M 1194.

Fig. 4



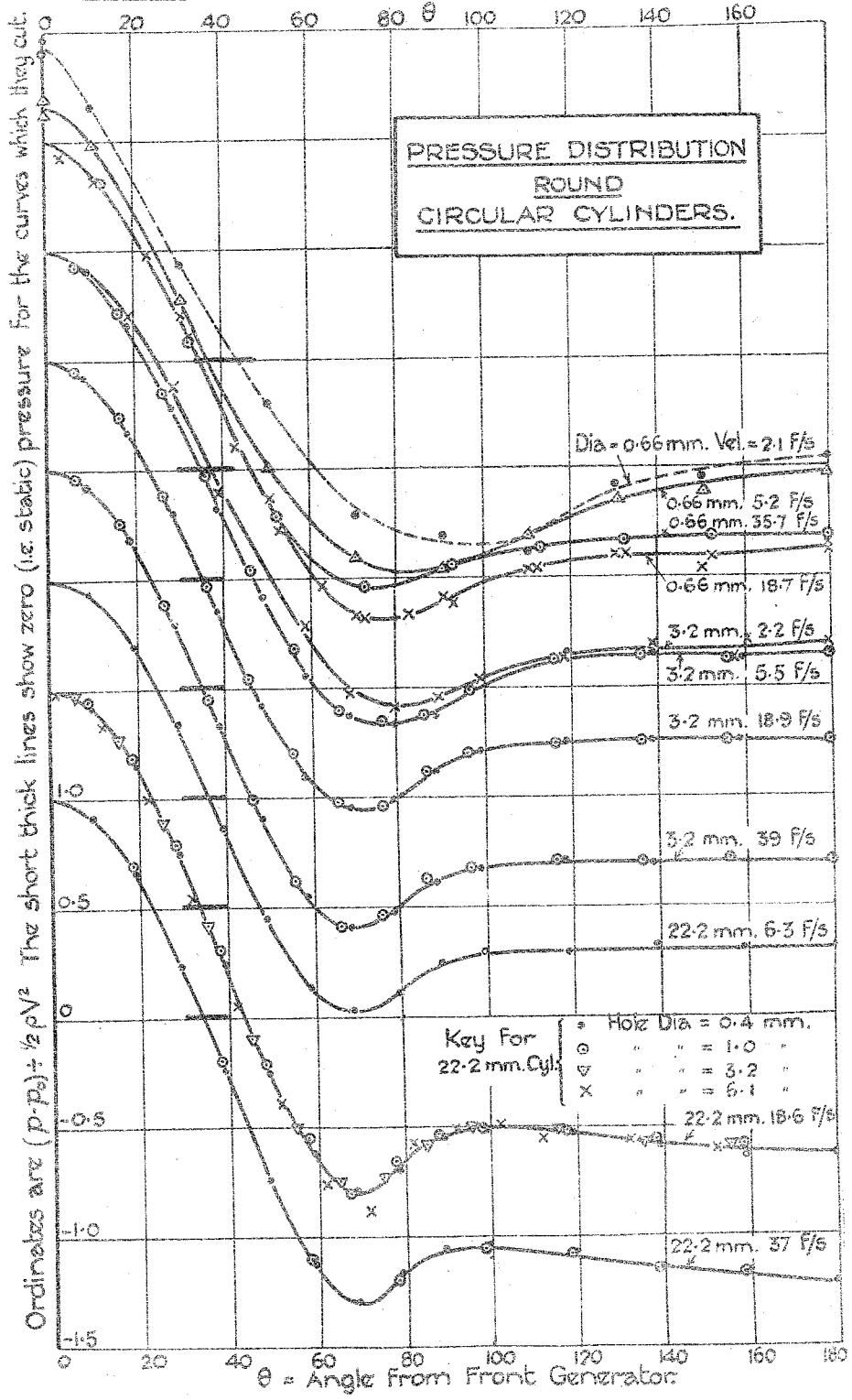
R. & M. 1194.

FIG. 5.



R & M. 1194.

Fig. 6.

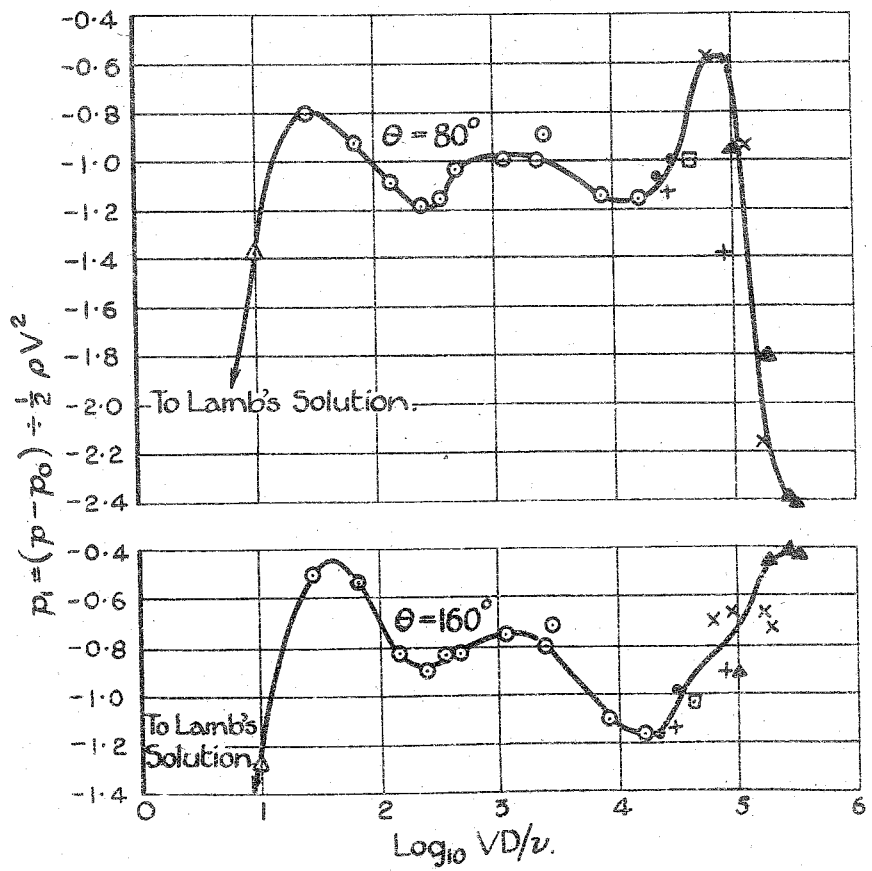


R.&M. 1194.

FIG. 7.

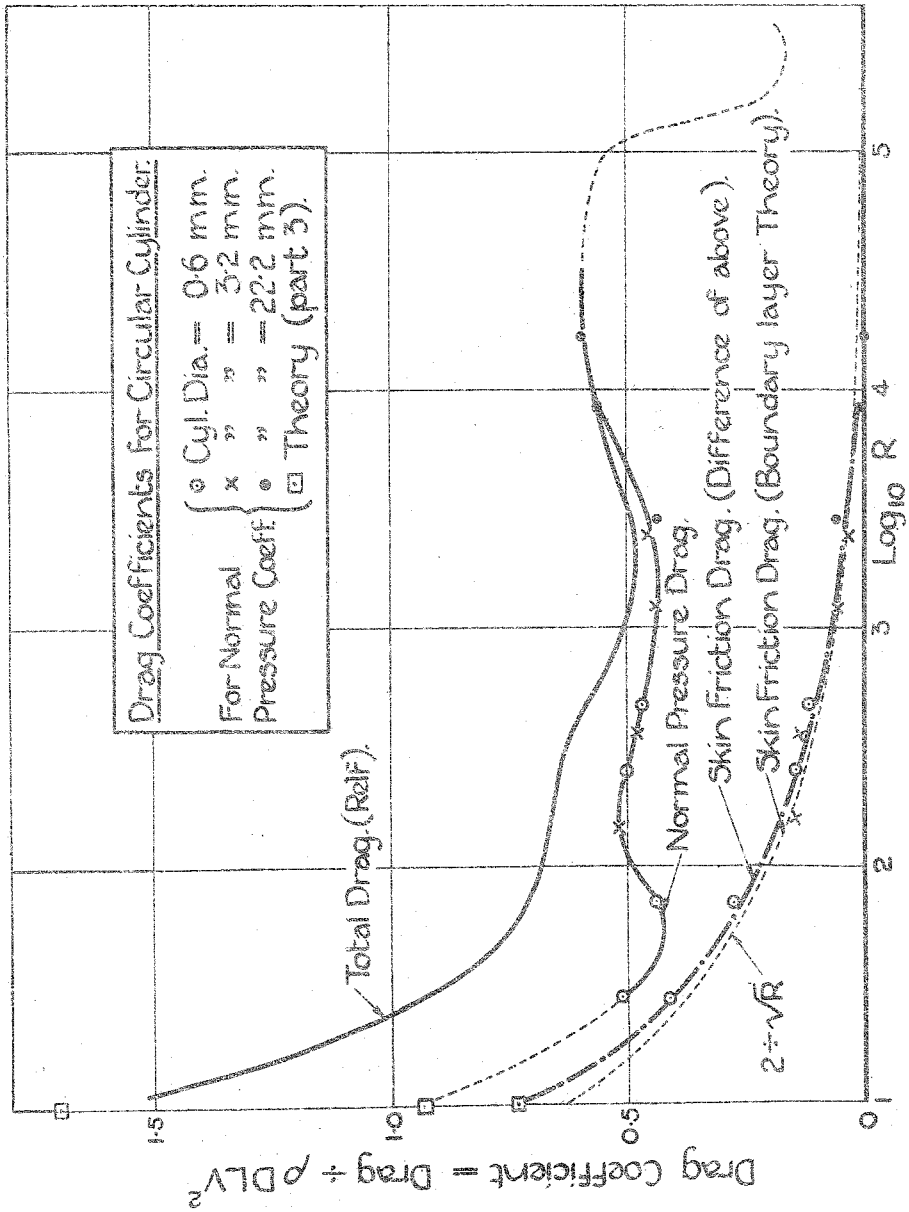
VARIATION OF PRESSURE WITH R, AT $\theta = 80^\circ$ & $\theta = 160^\circ$

- + — R.&M. N^o 1176.
- — Present Report (Expt.).
- △ — " " (Theory).
- — Fage.
- ▲ — " (Large Cylinder).
- x — Taylor. R.&M. N^o 191.
- — Parkins.



R. & M. 1194.

Fig. 9.

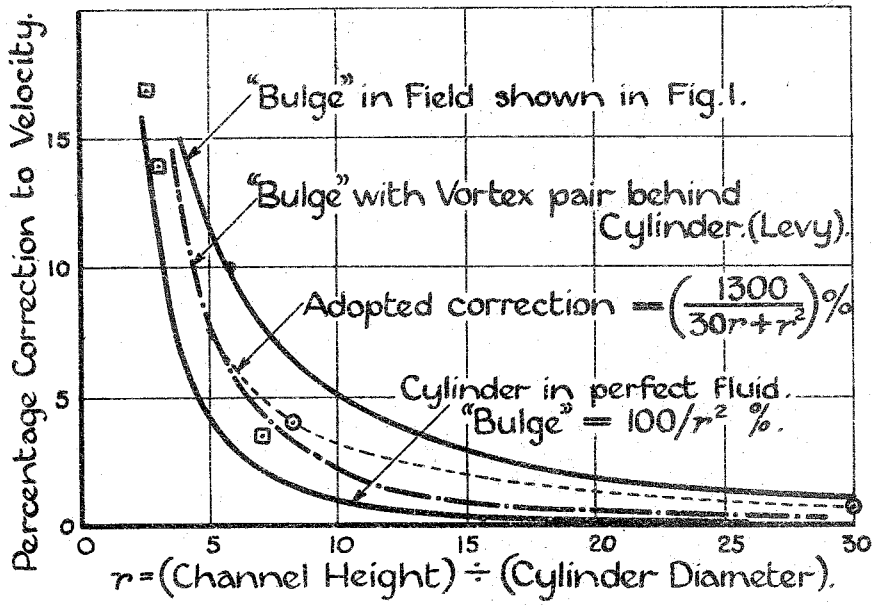


R. & M. 1194.

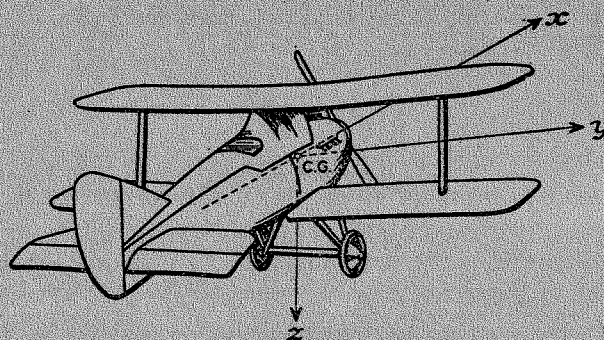
FIG. 10.

EFFECT OF CHANNEL WALLS.

- Wall Pressure Experiments.
- Parkin.
- Pressure Distribution R. & M. No 1176.



SYSTEM OF AXES.



Axis	Symbol Designation Positive } direction }	x longitudinal forward	y lateral starboard	z normal downward
Force	Symbol	X	Y	Z
Moment	Symbol Designation	L rolling	\pitchfork pitching	N yawing
Angle of Rotation	Symbol	ϕ	θ	ψ
Velocity	Linear	u	v	w
	Angular	p	q	r
Moment of Inertia		A	B	C

Components of linear velocity and force are positive in the positive direction of the corresponding axis. Components of angular velocity and moment are positive in the cyclic order y to z about the axis of x , z to x about the axis of y , and x to y about the axis of z .

The angular movement of a control surface (elevator or rudder) is governed by the same convention, the elevator angle being positive downwards and the rudder angle positive to port. The aileron angle is positive when the starboard aileron is down and the port aileron is up. A positive control angle normally gives rise to a negative moment about the corresponding axis. The symbols for the control angles are :-

- ξ aileron angle
- η elevator angle
- η_T tail setting angle
- ζ rudder angle

Recent Publications of the **AERONAUTICAL RESEARCH COMMITTEE**

*The publications named below can be purchased at the net prices shown
 (postage extra) from H.M. Stationery Office at the addresses
 shown on page 1 of cover, or through any bookseller :—*

T ECHNICAL REPORT of the Aeronautical Research Committee for the year 1924-25, with Appendices—	<i>s. d.</i>
Vol. I. Aeroplanes, Model and Full Scale - - -	17 6
Vol. II. Airscrews, Engines, Materials, etc. - - -	17 6
T ECHNICAL REPORT of the Aeronautical Research Committee for the year 1925-26 - - - - -	35 0
R EPORT of the Aeronautical Research Committee for the year 1925-26 - - - - -	2 0
R EPORT of the Aeronautical Research Committee for the year 1926-27 - - - - -	2 0

Reports & Memoranda. **LIST OF PUBLICATIONS.**

No. 650.	Reports and Memoranda of the Advisory Committee published on or before 31st March, 1920 - - -	<i>9d.</i>
„ 750.	Reports and Memoranda of the Aeronautical Research Committee published between 1st April, 1920 and 30th September, 1921 - - - - -	<i>2d.</i>
„ 850.	Reports and Memoranda of the Aeronautical Research Committee published between 1st October, 1921 and 31st March, 1923 - - - - -	<i>1d.</i>
„ 950.	Reports and Memoranda of the Aeronautical Research Committee published between 1st April, 1923 and 31st December, 1924 - - - - -	<i>4d.</i>
„ 1050.	Reports and Memoranda of the Aeronautical Research Committee published between 1st January, 1925 and 28th February, 1927 - - - - -	<i>4d.</i>
„ 1150.	Reports and Memoranda of the Aeronautical Research Committee published between 1st March, 1927 and 30th June, 1928 - - - - -	<i>4d.</i>

LIST OF PUBLICATIONS ON AERONAUTICS.*

- List B. Revised to 1st April, 1927.
- B.1. Air Ministry Publications.
- B.2. Aeronautical Research Committee Publications.

* This list may be obtained on application to H.M. Stationery Office.